Accepted Manuscript

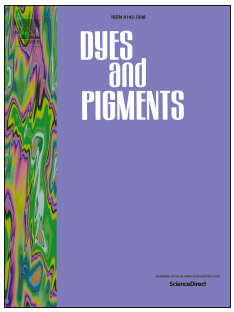

Self-assembly and anion-response of azobenzene-based L-valinamide derivative

Kechang Li, Pengchong Xue

PII: S0143-7208(17)32459-2

DOI: 10.1016/j.dyepig.2018.04.010

Reference: DYPI 6671

To appear in: *Dyes and Pigments*

Received Date: 1 December 2017

Revised Date: 30 March 2018

Accepted Date: 8 April 2018

Please cite this article as: Li K, Xue P, Self-assembly and anion-response of azobenzene-based L-valinamide derivative, *Dyes and Pigments* (2018), doi: 10.1016/j.dyepig.2018.04.010.

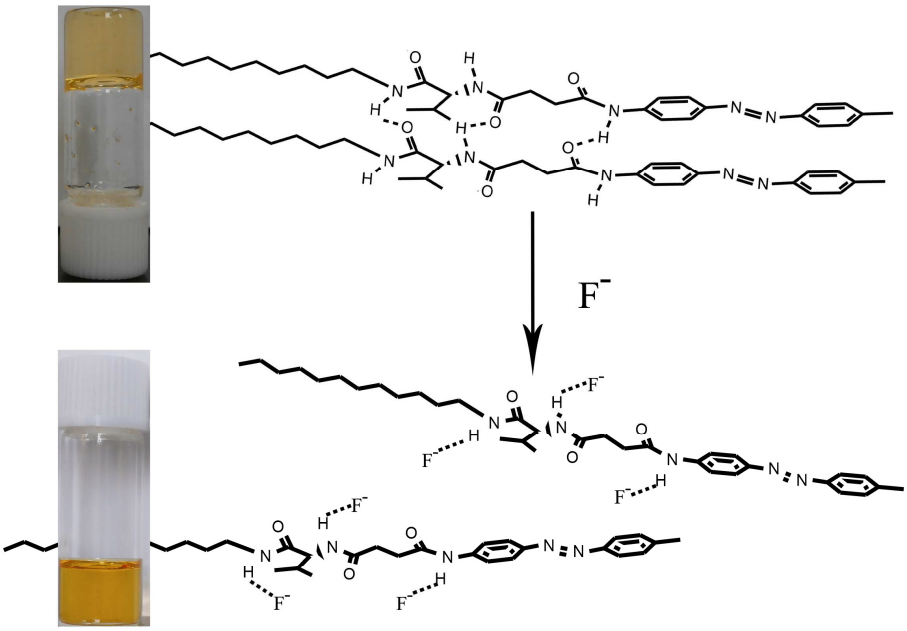

Self-assembly and anion-response of azobenzene-based L-valinamide derivative

Kechang Li,[a,*] Pengchong Xue[b]

[a] College of Chemistry, Jilin University, No. 2699, Qianjin Street, Changchun, 130012, P. R. China
[b] Tianjin Key Laboratory of Structure and Performance for Functional Molecules, Key Laboratory of Inorganic-Organic Hybrid Functional Material Chemistry, Ministry of Education, College of Chemistry, Tianjin Normal University, No. 393, Bin Shui West Road, Tianjin, 300387, P.R. China.

Abstract: An azobenzene-based L-valinamide derivative was synthesized, and its gelation ability and self-assembly in organic solvents were investigated. Results suggested that it is an excellent gelator and formed organogels in many solvents, such as 3-pentanone, aniline, *o*-dichlorobenzene (ODCB), CH_2Cl_2, THF, ethanol, DMSO, and DMF. Its self-assembly in ODCB gel was studied. Transmission electron microscopic observation suggested that the gelator can self-assemble into one-dimensional nanofibers in the gel, and this phenomenon is driven by hydrogen bonding between amide units and π-π interaction between azobenzene moieties. With the increase in gelator concentration, the gel-to-sol phase transition temperature increased and the gelation time of the solvent shortened. Moreover, the gel exhibit anion response. A gel-to-sol phase transition was found after fluoride anion was added, exhibiting selective response to F^-.

Keywords: gelator; self-assembly; anion; stimulus-response

1. Introduction

Supramolecular organogels formed by a low-molecular weight gelator recently attracted a growing attention because of their unique self-assemblies and wide applications. Different functional groups are appended to the molecular structures of gelators to impart specific applications, such as sensors (including gas,[5-8] anion,[9-10] cation[11-12] and neutral molecules[13]), drug releases systems,[14-15] medical treatments,[16-17] stimuli-responsive soft materials,[18-20] solar cell,[21] molecular recognition,[22] field effect transistors,[23] enantioselective sensing[24] and

* Corresponding author: likc@jlu.edu.cn

dyes absorbing.[25-26] Gelators form various assemblies, such as nanofibers, nanotubes, nanoribbons, nanorods, and plate-like structures, and the formation of these assemblies is driven by weak intermolecular interactions (van der Waals force, π-π interaction, hydrogen bonding, coordination, halogen bonding, and charge transfer interactions). These assemblies form a three-dimensional (3D) network to prevent solvent from flowing, resulting in gel formation. Generally, chiral carbon, hydrogen bonding moiety, and long alkyl chain are important factors that induce a gelator to self-assemble into a 3D network in different solvents.[27] A chiral center prevents molecules from orderly stacking and then forming large aggregation or deposition.[28] The hydrogen bonding groups may help a gelator to self-assemble into a 1D superstructure.[29-30] The long alkyl chain not only can adjust the solubility but also promotes crosslinking of 1D aggregate through nodes in coordination with the chiral center.[31]

In this work, based on the above designed principle, an L-valinamide derivative with dodecyl group as long alkyl chain, amide moieties as hydrogen bonding units and chiral center (**1**) was designed and synthesized. Its gelation ability and anion response were investigated. It was found to be an excellent gelator in many kinds of organic solvents, including aromatic hydrocarbon, ketone, aromatic amine, aromatic ketone, alcohol, chloroform, THF, and polar DMF, and DMSO. Moreover, its self-assembly in gel was investigated too. The results indicated that the gelator formed 1D nanofibers in gel. FT-IR and UV

absorption spectra revealed that the main driving forces of gel formation were hydrogen bonding and π-π interaction. Gelator concentration determined the gel-to-sol phase transition temperature (T_{gel}) and the gelation speed. Moreover, a gel-to-sol phase transition was observed upon the addition of fluoride anion.

2. Results and discussion

2.1 Synthesis of gelator 1

Compound **2** was synthesized in an aqueous solution as previously described.[32] The reaction of **2** and laurylamine in the presence of EDC·HCl in dry CH_2Cl_2 yielded compound **3**. A deprotection process of **3** by diethylamine provided compound **4** with a moderate yield (78%). Compound **6** could be easily obtained through an amidation reaction of **5** with succinic anhydride at a yield of 93%. Compound **1** was prepared via a condensation reaction of **4** and **6**, producing a moderate yield (66%).

2.2 Gelation ability

Through a standard heating and cooling method,[33] the gelation ability of **1** was investigated, and the results are listed in Table 1. Compound **1** is insoluble or has a low solubility in measured solvents at room temperature and poorly soluble in nonpolar alkane (such as hexane and cyclohexane), petroleum ether, acetone, benzene, and toluene even upon heating. Although **1** dissolves in ethyl acetate upon heating, only yellowish deposition was observed when the solution was cooled to room temperature. Fortunately, the gel phases in other

solvents were formed while the hot solution cools. The gelation solvents include aromatic solvents, for instance mesitylene and *o*-dichlorobenzene (ODCB), aromatic amines, and aromatic ketone. Stable gels formed in CH_2Cl_2, $CHCl_3$, THF, and ethanol with low boiling points. Moreover, **1** can gelate DMSO and DMF. The above results clearly indicated that the long alkyl chain and chiral amino acid indeed rendered **1** an excellent gelator of many organic solvents.

Table 1. Gel properties of **1** in organic solvents.[a]

Solvent	Status[b]	Solvent	Status
Hexane	I	Aniline	TG
Cyclohexane	I	N-Methylaniline	TG
Petroleum ether	I	N-Dimethylaniline	TG
Ethyl acetate	I	CH_2Cl_2	TG
Acetone	P	$CHCl_3$	TG
3-Pentanone	OG	THF	TG
2,4-Dimethylpentanone	OG	Ethanol	OG
Benzene	I	Acetophenone	TG
Toluene	I	DMF	OG
Mesitylene	TG	DMSO	TG
o-Dichlorobenzene	TG	Benzyl alcohol	TG

[a] TG : transplant gel; OG: opaque gel; S: soluble; I: insoluble; P: precipitate. [b] Gelator = 5.0 mg/mL.

2.3 Gel-to-sol phase transition temperature

When the formed gels were heated to a given temperature and transformed into a sol, this temperature was defined as T_{gel}.[34] While the hot sol was cooled to room temperature, a gel phase reappeared, demonstrating thermal reversibility. Here, the influence of gelator concentration on T_{gel} was examined. Fig. 1a shows the relationship between T_{gel} and gelator concentration. T_{gel} values increase nonlinearly with increasing gelator concentration. T_{gel} reaches 78 ºC

when concentration is 1.0 mg/mL. The system with a concentration of 2.5 mg/mL did not maintain a gel phase when the temperature increased to 94 °C. If the gel-to-sol transition is comparable to the melting of crystals, the phase transition enthalpy can be estimated by the following equation:

$$1/T_{gel} = R\frac{lnC}{\Delta H} + \frac{\Delta S}{\Delta H}$$

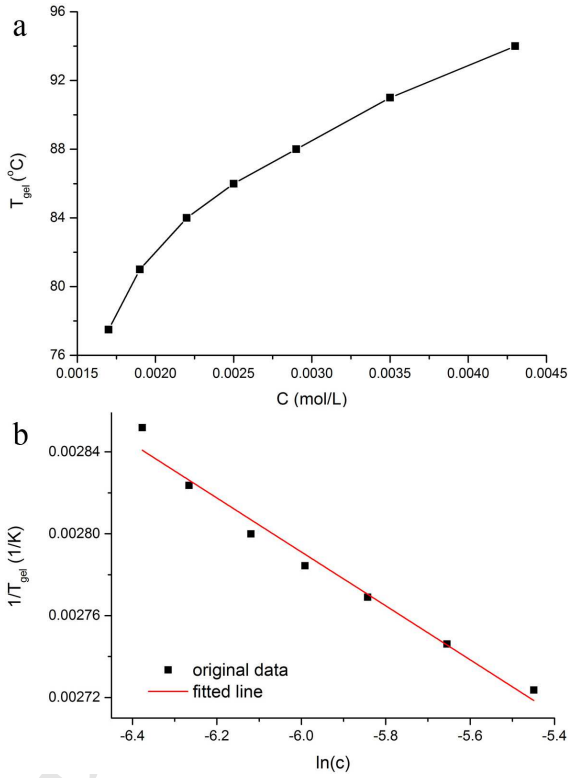

Fig. 1. Plots of (a) T_{gel} versus concentration of **1** and (b) $1/T_{gel}$ versus the natural logarithm of the concentration of **1** in ODCB.

where C is the molar gel concentration, *ΔH* and *ΔS* are the standard enthalpy and entropy for the sol–gel transition, respectively, and R is the gas constant.[35-37] The reciprocal melting temperature was linearly dependent on the natural logarithm of the concentration (Fig. 1b). Based on the fitted linear equation, *ΔH* and *ΔS* were -6.31×10^4 J mol^{-1} (–109.4 J g^{-1}) and -126.2 J mol^{-1}

K^{-1}. The Gibbs free-energy change ΔG and the aggregation constant K at room temperature were –25.5 kJ mol^{-1} and 2.89 × 10^4 M^{-1}, respectively. Such a moderate aggregation constant is possibly responsible for the good gelation abilities of **1** in many solvents.[38]

2.4 Morphological observation

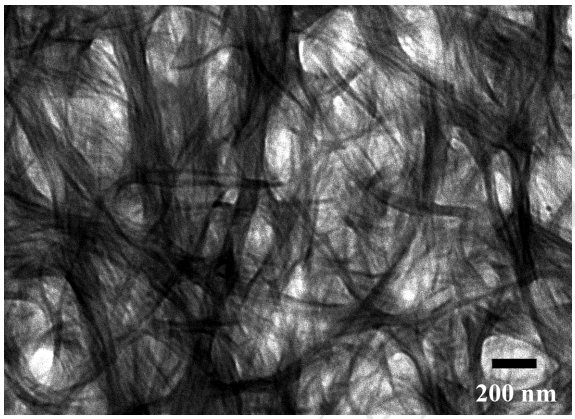

Fig. 2. TEM image of ODCB xerogel.

To observe the morphology of self-assemblies of the gel phases of 1, we obtained a transmission electron microscopic (TEM) image of the xerogel film. Fig. 2 shows the TEM image of ODCB xerogel, in which long nanofibers with widths of 25-100 nm are observed. Moreover, wide fibers consist of thin fibers. This result suggests that 1 tends to self-assemble to from 1D aggregate in the gel phase.[39]

2.5 FT-IR and ^{1}H NMR spectra

As discussed above, amide moieties may promote the formation of 1D aggregate through intermolecular hydrogen bonding; we thus obtained the FT-IR spectrum of xerogel film. As shown in Fig. 3, the stretching vibrational peak of N-H is located at 3288 cm^{-1}. The vibration peaks at 1664 and 1635 cm^{-1} are assigned to the aromatic

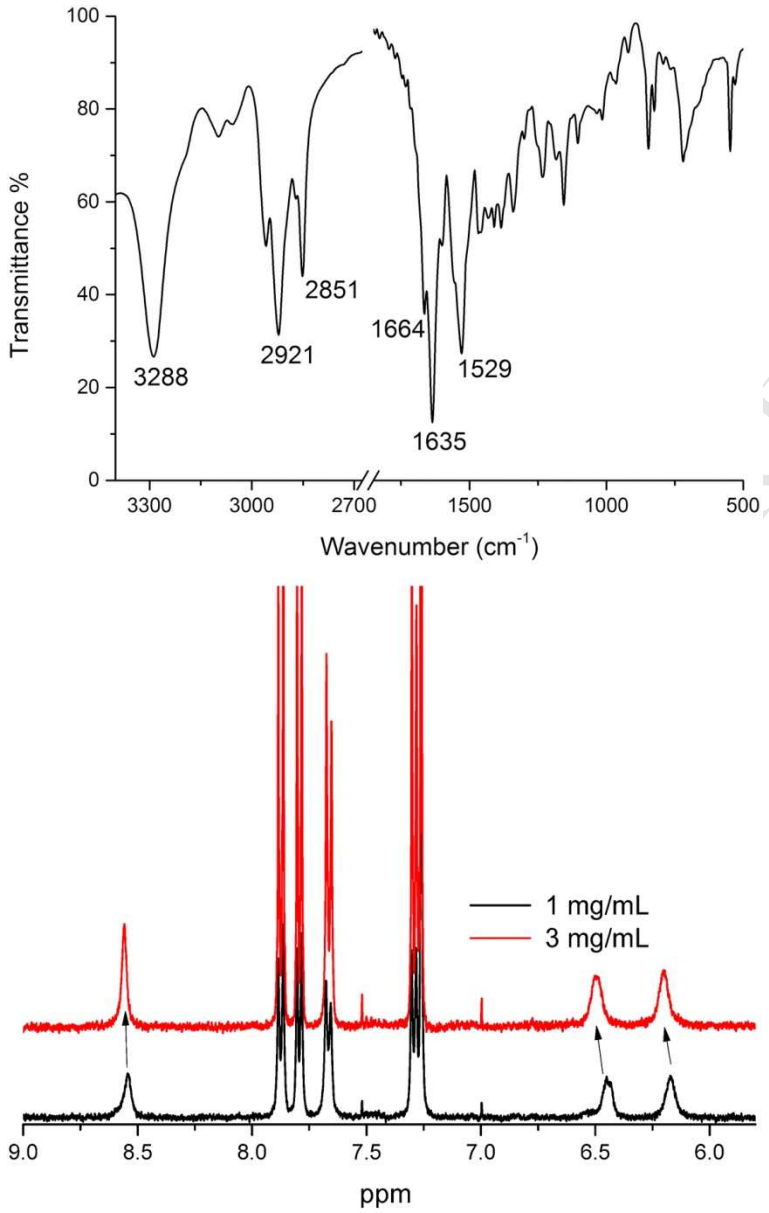

Fig. 3. (a) FT-IR spectrum of ODCB xerogel film, and (b) concentration-dependent NMR spectra in $CDCl_3$.

and aliphatic C=O vibrational peaks, respectively.[40] The locations of these vibrational peaks indicate that all of the amide groups are involved in hydrogen bonding.[41] In addition, the antisymmetric and symmetric stretching vibrational bands of CH_2 in xerogel film are located at 2921 and 2851 cm^{-1}, respectively, implying that the alkyl chains adopt an all-trans extended conformation,[42] and the van der Waals interaction among the alkyl chains plays an important role in the self-assembly of **1**. IR spectral

results also reveal that intermolecular hydrogen bonding is a major driving force in gel formation. In addition, the IR spectrum of the as-synthesized solid was measured and found to be the same as that of gel, indicating that there is intermolecular hydrogen bonding in as-synthesized solid. Fig. 3b shows the concentration-dependent NMR spectra in $CDCl_3$. It is clear that the peaks ascribed to three N-H groups in higher concentration shifted to low field. This result suggests that hydrogen bonding in higher concentration became stronger relative to those in low concentration.

2.6 UV-Vis spectral change during gelation.

To monitor the interaction between azobenzene moieties during gelation, we investigated the UV-Vis absorption spectral change of **1** in ODCB during gelation. As shown in Fig. 4a, the maximal absorption peak in the hot solution is located at 355 nm and slightly increased and red-shifted to 357 nm after **1** min; this phenomenon is ascribed to planarization of azobenzene moiety.[43] This peak rapidly decreased with time and remained nearly unchanged after 10 min. Moreover, a new peak at 314 nm, which is ascribed to aggregates, appeared and gradually increased during gelation. An isoabsorptive point at 326 nm was observed, suggesting an equilibrium reaction of the two components. The disappearance of the peak at 357 nm and the appearance of a new peak at 314 nm clearly revealed a large blueshift of 43 nm, suggesting that the gelators stack together in a face-to-face H-aggregate.[44] Moreover, absorption spectral shift of 41 nm illustrates that strong π-π interactions exist between azobenzene moieties, which is a main driving force for molecular aggregation in organic

solvents. Based on these results, a suggested packing process for **1** during gelation is shown in Fig. 5. Molecules as monomers exist in hot solution. During gelation molecules stack together in a parallel fashion and all three amide groups are involved in intermolecular hydrogen bonding. A gelator forms six hydrogen bonds with two adjacent gelators. Moreover, azobenzene moieties form H-aggregates through hydrogen bonding. In addition, XRD spectrum was measured, but no obvious diffraction peaks were observed. So, stacking model in the long-distance period is unknown.

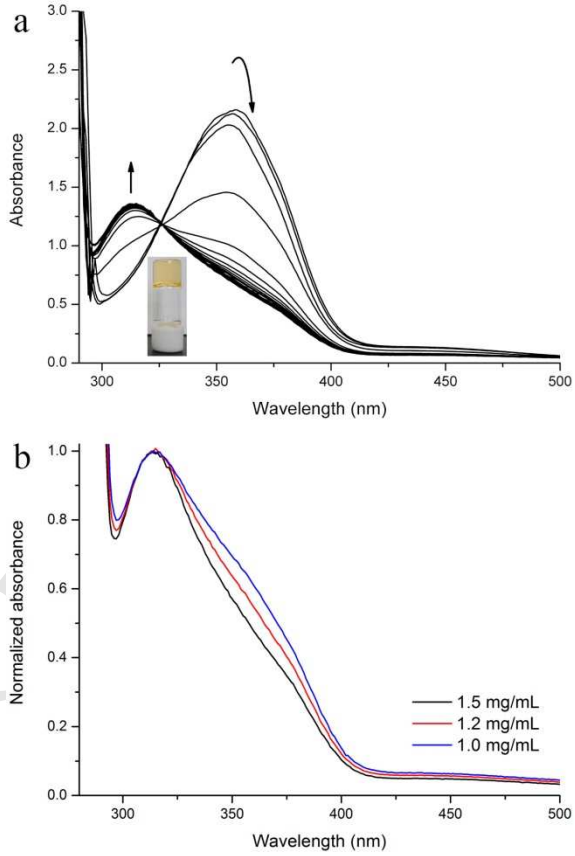

Fig. 4. (a) UV/Vis absorption spectral changes during gelation in ODCB (1.5 mg/mL) with an interval of **1** min as the hot solution was cooled from 100 °C to 20 °C. Inset is the photo of ODCB gel. (b) Normalized absorption spectra of **1** in gels with different concentrations.

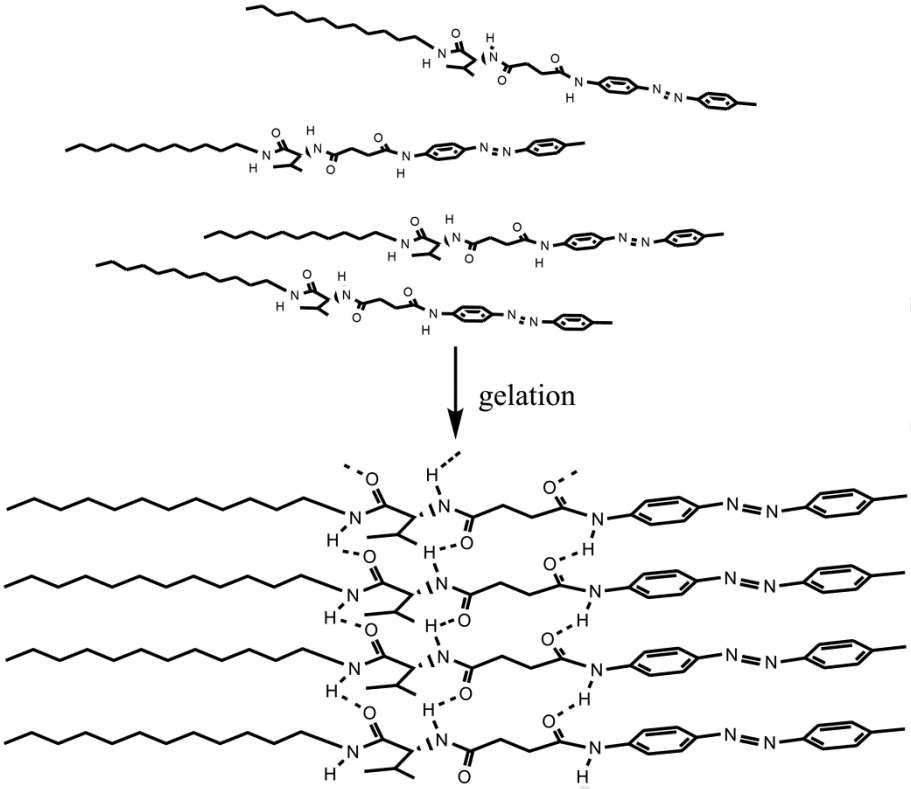

Fig. 5. Schematic of possible packing of **1** during gelation.

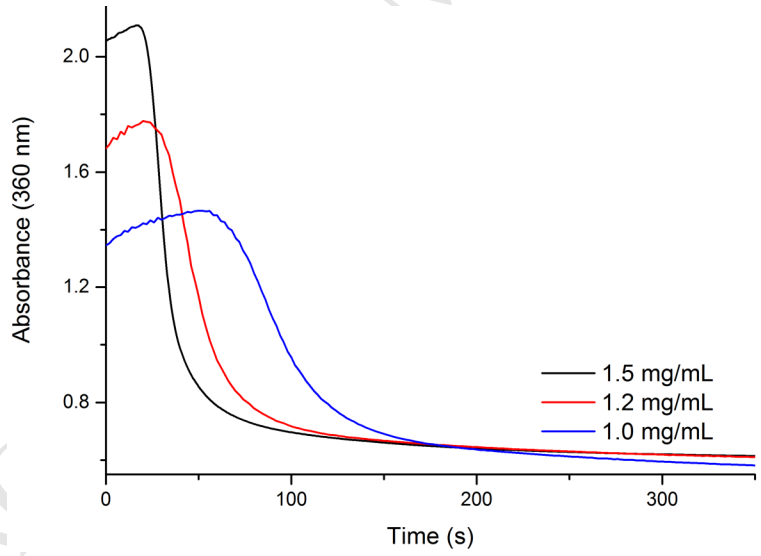

Fig. 6. Dynamic changes of absorbance of **1** at 360 nm during gelation at different concentrations. The sample firstly was heated to 120 ºC and then cooled naturally to room temperature.

Fig. 4b shows the normalized absorption spectra of gels in different ODCB concentrations. The absorbance at around 350 nm from monomeric molecules gradually weakened with increasing concentration. This result suggests that the proportion of monomeric molecules relative to that of aggregates decreases under increased concentration. Furthermore, the gelation speed of **1** in ODCB was dependent on the concentration of the compound. As shown in Fig. 6, the absorbance at 360 nm at a concentration of 1.5 mg/mL increases first within 18 s and then rapidly decreases. When the concentration decreases to 1.2 mg/mL, the arising time in absorbance extends to 20 s, and the descending rate of the absorbance slows down, indicating a slow gelation process. If the concentration further decreases to 1.0 mg/mL, the absorbance slowly starts down after 52 s. These results imply that a low gelator concentration requires a low temperature to form gel, resulting in a slow gelation speed.

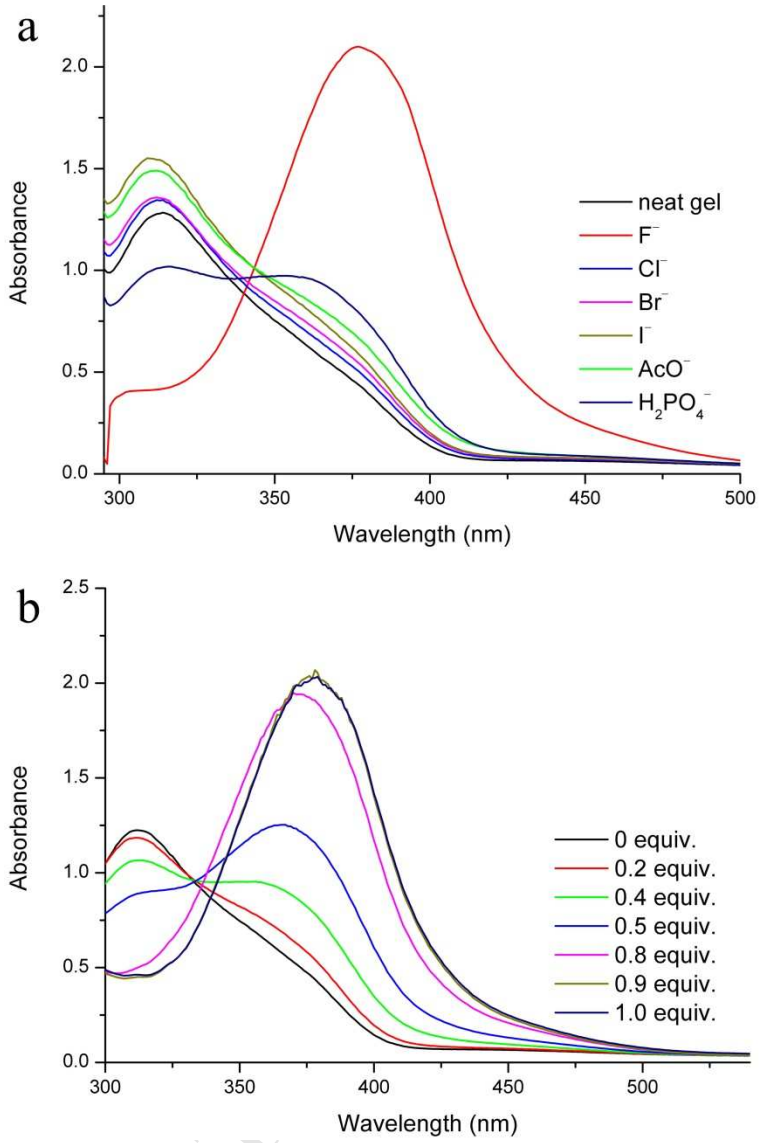

Fig. 7. Absorption spectra of **1** in ODCB (1.0 mg/mL) upon addition of (a) 1 equiv. different anions and (b) in presence of fluoride anions with different concentrations.

2.7 Anion response of gel

The anion responsive properties of **1** gel toward different anions (F^-, Cl^-, Br^-, I^-, AcO^- and $H_2PO_4^-$ as tetrabutylammonium (TBA) salts) were examined in DMSO. It was found that the gel was destroyed and changed into a sol when the TBAF solution was added on surface of gel and stayed for 1 h. However, other TBA salts did not induce such phase transition. Moreover, fluoride anion

can prevent the gel formation. The hot solution of **1** (1.0 mg/mL) in ODCB could not be changed into a gel upon the addition of 1 equiv. TBAF even when the solution was left over one day. The gel state of **1** in ODCB could be maintained after adding the same amount of other halide anions. It suggests that the anions, not the TBA cation, should be responsible for the phase transition from a gel to a sol.[10b] Absorption spectra were further used to investigate this phenomenon. As shown in Fig. 7a, the absorption spectra in the presence of Cl^-, Br^-, I^-, AcO^- are similar to that of the neat gel. The absorption peak at 314 nm, ascribing to H-aggregate, disappeared in the presence of 1.0 equiv F^-, and a new peak at 378 nm emerged. This result suggests that F^- may destroy the molecular aggregate.[46] The absorption peak at 314 nm decreased and the absorption at 360 nm emerged while 1.0 equiv. $H_2PO_4^-$ existed, indicating that $H_2PO_4^-$ could partly destroy aggregate. In addition, it was found that a sol phase was observed when 5.0 equiv. $H_2PO_4^-$ existed, suggesting that $H_2PO_4^-$ may destroy a gel phase in higher concentration. Because the absorption peak located at 357 nm in hot solution, meaning a small red-shift of 21 nm, the hydrogen bonding between amide and F^- should be responsible for the dissociation of gelator's aggregate. The reason of selective response to fluoride anion is due to weaker ability of other anions to form hydrogen bond with amide group. Furthermore, the F^- concentration strongly impacted the phase transition. When the ratio of F^- to **1** was lower than 0.5, a gel phase could be still kept. Fig. 7b shows the concentration-dependent absorption spectra. The

absorption band at 314 nm gradually decreased and the absorbance at more than 365 nm gradually increased upon the addition of TBAF. While the ratio of F^- to **1** reached 0.5, the peak intensity at 366 nm was stronger than that at 314 nm. At the moment, there were enough fibrous aggregates to hold a gel phase. As a result, only a sol was observed.

Conclusions

An azobenzene-based L-valinamide derivative bearing a long alkyl chain, chiral carbon, and amide moieties was synthesized, and the self-assembly of this compound into a gel was investigated. The results indicate that the synthesized compound is an excellent gelator and can form gels in various organic solvents, such as, aromatic solvents, ketone, alcohols, halohydrocarbons, THF, DMF, and DMSO. The gelator may self-assemble into nanofiber in gels, and this process is driven by multiple hydrogen bonds and π-π interactions. T_{gel} and gel speed are strongly dependent on gelator concentration. Moreover, the gel exhibited selective response to fluoride anion. The addition of fluoride anion could result in a gel-to-sol phase transition. Our findings suggest that introduction of long alkyl chain, chiral carbon, and amide groups render a compound to be an excellent gelator and the existence of amide group may promote a gel to response anions.

Experiment section

Instruments and experimental methods: All the raw materials were used without further purification. All the solvents as analytical reagents were purchased from Beijing Chemical Works (Beijing, China), and were used without further purification. Infrared spectra were measured with a Nicolet- 360 Fourier transform infrared (FT-IR) spectrometer by incorporating the samples in KBr disks. The UV-vis spectra were determined on a Mapada UV-1800pc spectrophotometer. C, H, and N elemental analyses were performed on a Perkin-Elmer 240C elemental analyzer. ^{1}H NMR spectra were recorded on Mercury plus 500 MHz.

TEM investigation: A piece of the gels was placed on a carbon-coated copper grid (400 mesh) followed by naturally evaporating the solvent. The TEM specimens were examined with a Hitachi mode H600 A-2 apparatus with an accelerating voltage of 100 kV.

Gelation test of organic fluids: The solution of gelator (pre-weighed) in organic solvent was heated in a sealed test tube (diameter = 1 cm) in an oil bath until the solid was dissolved. The solution was allowed to stand at room temperature for 6 h, and the state of the mixture was evaluated by the “stable to inversion of a test tube” method.

Light response of gel: The gel at a concentration of 1.0 mg/mL was prepared in a cell with 1 mm optical path, aged for 6 h and inverted, and then exposed to a high pressure mercury lamp (500 W) with a 365 nm filter. UV-vis absorption spectra of the gels before and after illumination were measured.

Gelator synthesis:

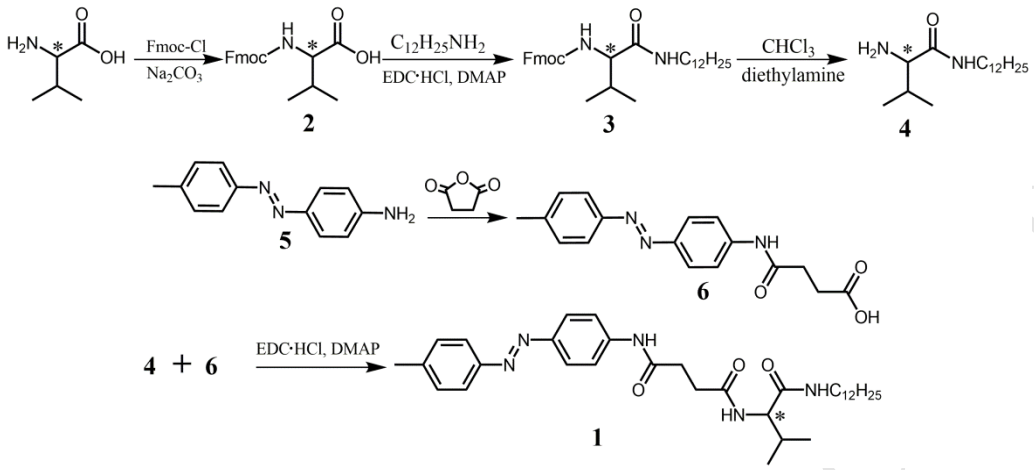

Scheme 1. Synthesis route of **1**.

N-Fmoc-L-valine (**2**) and **5** were synthesized by the reported procedure.[45,46]

(S)-(9H-fluoren-9-yl)methyl-1-(dodecylamino)-3-methyl-1-oxobutan-2-ylcarbamate (**3**)

N-Fmoc-L-valine (2.79 g), DMAP (0.2 g) and laurylamine (1.58 g) were dissolved in 100 mL dried CH_2Cl_2. EDC·HCl (2.0 g) was added into the above solution at 0 ºC. The mixture was stirred at room temperature for 24 h. After the solvent was removed, ethanol (100 mL) was added and the mixture was treated for 5 min in an ultrasonic cleaner. The compound was obtained by filtration and washing with ethanol. Yield = 71%. mp = 146-148 ºC. FT-IR (cm^{-1}): 3219, 3065, 2956, 2920, 2851, 1692, 1648, 1549, 1250, 740. ^{1}H NMR (500 MHz, $CDCl_3$): δ 7.76 (d, J = 7.5 Hz, 2H), 7.59 (d, J = 7.5 Hz, 2H), 7.40 (t, J = 7.5 Hz, 2H), 7.31 (td, J = 7.5, 1.1 Hz, 2H), 5.77 (s, 1H), 5.37 (d, J = 8.9 Hz, 1H), 4.40 (dt, J = 17.6, 10.4 Hz, 2H), 4.22 (t, J = 6.9 Hz, 1H), 3.88 (t, J = 7.8 Hz, 1H), 3.45 – 3.04 (m, 2H), 2.21 – 2.01 (m, 1H), 1.49 (t, J = 7.3 Hz, 2H), 1.34–1.18

(m, 18H), 0.95 (t, J = 7.2 Hz, 6H), 0.88 (t, J = 7.0 Hz, 3H). Element analysis for $C_{32}H_{46}N_2O_3$: C, 75.85; H, 9.15; N, 5.53; found: C, 75.82; H, 9.19; N, 5.51.

(S)-2-amino-N-dodecyl-3-methylbutanamide (**4**)

3 (2.0 g) and diethylamine (5 mL) was dissolved in CH_2Cl_2 (20 mL) and the mixture was heated for 1 h at 50 ºC. After the solvent was removed and the residues was treated by column chromatography (silica, CH_2Cl_2/methanol = 10/1 (V/V)). Yield = 78 %. mp = 44-46 ºC. FT-IR (cm^{-1}): 3372, 3297, 3087, 2954, 2850, 1642, 1556, 1463. ^1H NMR (500 MHz, $CDCl_3$): δ 3.24 (m, 3H), 2.31 (m, 1H), 1.50 (p, J = 7.2 Hz), 1.35-1.21 (m, 18H), 0.99 (d, J = 7.0 Hz, 3H), 0.88 (t, J = 6.8 Hz, 3H), 0.83 (d, J = 6.9 Hz, 3H). Element analysis for $C_{17}H_{35}N_2O$: C, 72.03; H, 12.44; N, 9.88; found: C, 72.07; H, 12.41; N, 9.89.

(E)-4-oxo-4-(4-(p-tolyldiazenyl)phenylamino)butanoic acid (**6**)

5 (0.5 g, 2.4 mmol) and succinic anhydride (0.5 g, 5.0 mmol) were dissolved in dried THF (10 mL) and the mixture were refluxed 24 h. The solvent was removed, 10 ml $CHCl_3$ was added and the mixture was treated for 5 min in an ultrasonic cleaner. The solid was obtained by filtration. Yield: 93%. mp = 205-206 ºC. FT-IR (cm^{-1}): 3430, 3309, 3042, 2925, 1718, 1668, 1594, 1533, 844. ^1H NMR (500 MHz, DMSO-d_6): δ 12.15 (s, 1H), 10.31 (s, 1H), 7.85 (d, J = 7.6 Hz, 2H), 7.80 (d, J = 8.6 Hz, 2H), 7.76 (d, J = 6.8 Hz, 2H), 7.38 (d, J = 7.7 Hz, 2H), 3.32 (s, 2H), 2.62 (t, J = 6.5 Hz, 3H), 2.55 (t, J = 6.5 Hz, 3H), 2.40 (s, 4H). Element analysis for $C_{17}H_{17}N_3O_3$： C, 65.58; H, 5.50; N, 13.50; found: C, 65.50; H, 5.55; N, 13.49.

(E)-N1-(1-(dodecylamino)-3-methyl-1-oxobutan-2-yl)-N4-(4-(p-tolyldiazenyl)phenyl)succinamide (**1**)

4 (0.23 g，0.8 mmol), **6** (0.26 g，0.84 mmol) and a small amount of DMAP were dissolved in 20 mL dried THF. EDC·HCl (0.2 g) was added into the above solution at 0 ºC. The mixture was stirred at room temperature for 48 h. The compound was obtained by filtration and then washing with ethanol. Yield = 66%. mp = 237-239 ºC. FT-IR (cm^{-1}): 3288, 3098, 2958, 2921, 2851, 1664, 1635, 1528, 845. ^{1}H NMR (500 MHz, DMSO-d_6): δ 10.31 (d, 1H) , 7.91 (d, J = 8.9 Hz, 1H), 7.85 (d, J = 8.6 Hz, 2H), 7.80 (d, J = 8.7 Hz, 3H), 7.77 (d, J = 8.1 Hz, 2H), 7.39 (d, J = 8.0 Hz, 2H), 4.09 (t, J = 7.9 Hz, 1H), 3.17 – 2.91 (m, 2H), 2.63 (m, 2H), 2.54 (m, 2H), 2.41 (s, 3H), 1.99 (m, 1H), 1.37 (m, 2H), 1.32-1.14 (m, 18H), 0.84 (m, 9H). Element analysis for $C_{34}H_{51}N_5O_3$： C, 70.68; H, 8.90; N, 12.12; found: C, 70.73; H, 8.78; N, 12.17.

Acknowledgements

This work was financially supported by the National Natural Science Foundation of China (21103067), the Youth Science Foundation of Jilin Province (20130522134JH).

Notes and references

1. Jones CD, Steed JW. Gels with sense: supramolecular materials that respond to heat, light and sound. Chem Soc Rev 2016;45:6546–96.

2. Babu SS, Praveenn VK, Ajayaghosh, A. Functional π-gelators and their applications. Chem Rev 2014;114:1973–2129

3. Praveen VK, Ranjith C, Bandini E, Ajayaghosh A, Armaroli N, Oligo (phenylenevinylene) hybrids and self-assemblies: versatile materials for excitation energy transfer. Chem Soc Rev 2014;43:4222–42.

4. Jintoku H, Yamaguchi M, Takafuji M, Ihara H. Molecular gelation–induced functional phase separation in polymer film for energy transfer spectral conversion. Adv Funct Mater 2014;24:4105–12.

5. Xue P, Sun J, Yao B, Gong P, Zhang Z, Qian C et al. Strong emissive nanofibers of organogels for the detection of volatile acid vapors. Chem Eur J 2015;21:4712–20.

6. Fan J, Chang X, He M, Shang C, Wang G, Yin S et al. Functionality-oriented derivatization of naphthalene diimide: a molecular gel strategy-based fluorescent film for aniline vapor detection. ACS Appl Mater Interfaces 2016;8:18584–92.

7. Xue P, Yao B, Sun J, Zhang Z, Lu R. Emission enhancement of a coplanar p-conjugated gelator without any auxiliary substituents. Chem Commun 2014;50:10284–6.

8. Sun Y, Wang Y, Wu M, Yuan W, Chen Y. p-Quaterphenylene as an aggregation-induced emission fluorogen in supramolecular organogels and fluorescent sensors. Chem Asia J 2017;12:52–9.

9. Xu Y, Li C, Cao Q, Wang B, Xie Y. A pyrenyl-appended organogel for fluorescence sensing of anions. Dyes Pigm 2017;139:681–7.

10. (a) Sarma RJ, Devia K. Cystine-derived bis-naphthalimides as stimuli-responsive fluorescent gelators. New J Chem, 2015;39:4375–83; (b) Bai B, Zhang M, Wei J, Yan H, Wang H, Wu Y, Li M. Stimuli-responsive organogels based on a gelator of hydrazide and azobenzene units connected via a flexible central spacer. Tetrahedron 2016;72:5363-8.
11. Yao H, Wu H, Chang J, Lin Q, Wei T, Zhang Y. A carboxylic acid functionalized benzimidazole-based supramolecular gel with multi-stimuli responsive properties. New J Chem, 2016;40:4940–4.
12. Wang Y, Wang Z, Xu Z, Yu X, Zhao K, Li Y, Pang X. Ultrasound-accelerated organogel: application for visual discrimination of Hg^{2+} from Ag^{+}. Org Biomol Chem 2016;14:2218–22.
13. Zhang L, Jin Q, Liu M. Enantioselective recognition by chiral supramolecular gels. Chem Asian J 2017;11:2642-9.
14. Basu K, Baral A, Basak S, Dehsorkhi A, Nanda J, Bhunia D, et al. Peptide based hydrogels for cancer drug release: modulation of stiffness, drug release and proteolytic stability of hydrogels by incorporating D-amino acid residue(s). Chem Commun 2016;52:5045-8
15. Martin C, Oyen E, Wanseele YV, Haddou TB, Schmidhammer H, Andrade J et al. Injectable peptide-based hydrogel formulations for the extended in vivo release of opioids. Mater Today Chem, 2017;3:49-59.
16. (a) Du X, Zhou J, Shi J, Xu B. Supramolecular hydrogelators and hydrogels: from soft matter to molecular biomaterials. Chem Rev 2015;115:13165-307;

(b) Shigemitsu H, Hamachi I. Design strategies of stimuli-responsive supramolecular hydrogels relying on structural analyses and cell-mimicking approaches. Acc Chem Res 2017;50:740-50.

17. (a) Vargiu AV, Iglesias D, Styan KE, Waddington LJ, Eastonc CD, Marchesan S. Design of a hydrophobic tripeptide that self-assembles into amphiphilic superstructures forming a hydrogel biomaterial. Chem Commun, 2016;52:5912-5; (b) Feng Z, Wang H, Zhou R, Li J, Xu B. Enzyme-instructed assembly and disassembly processes for targeting downregulation in cancer cells. J Am Chem Soc 2017;139:3950-3; (c) Wang Z, Zhang F, Wang Z, Liu Y, Fu X, Jin A et al. Hierarchical assembly of bioactive amphiphilic molecule pairs into supramolecular nanofibril self-supportive scaffolds for stem cell differentiation. J Am Chem Soc 2016;138:15027-34; (d) Zhan J, Cai Y, Ji S, He S, Cao Y, Ding D, et al. Spatiotemporal control of supramolecular self-assembly and function. ACS Appl Mater Interfaces 2017;9:10012-8.
18. Chen C, Chen J, Wang T, Liu M. Fabrication of helical nanoribbon polydiacetylene via supramolecular gelation: circularly polarized luminescence and novel diagnostic chiroptical signals for sensing. ACS Appl Mater Interfaces 2016;8:30608-15.
19. Yu X, Chen L, Zhang M, Yi T. Low-molecular-mass gels responding to ultrasound and mechanical stress: towards self-healing materials. Chem Soc Rev, 2014;43:5346-71.

20. (a) Gao S, Wang S, Ma J, Wu Y, Fu X, Marella RK, et al. Salt tunable rheology of thixotropic supramolecular organogels and their applications for crystallization of organic semiconductors. Langmuir 2016;32:12805-13;

(b) Lee JH, Jung SH, Lee SS, Kwon K, Sakurai K, Jaworski J et al. Ultraviolet patterned calixarene-derived supramolecular gels and films with spatially resolved mechanical and fluorescent properties. ACS Nano 2017;11:4155-64.

21. (a) Tevis ID, Tsai W, Palmer LC, Aytun T, Stupp SI. Grooved nanowires from self-assembling hairpin molecules for solar cells. ACS Nano 2012;6:2032–40; (b) Yu Z, Qin D, Zhang Y, Sun H, Luo Y, Meng Q et al. Quasi-solid-state dye-sensitized solar cell fabricated with poly (β-hydroxyethyl methacrylate) based organogel electrolyte. Energy Environ Sci 2011;4:1298-305; (c) Park S, Song IY, Lim J, Kwon YS, Choi J, Song S et al. A novel quasi-solid state dye-sensitized solar cell fabricated using a multifunctional network polymer membrane electrolyte. Energy Environ Sci 2013;6:1559-64; (d) Xue P, Xu Q, Gong P, Qian C, Zhang Z, Jia J et al. Two-component gel of a D–π–A–π–D carbazole donor and a fullerene acceptor. RSC Adv 2013;3:26403-11; (e) Xue P, Lu R, Zhao L, Xu D, Zhang X, Li K et al. Hybrid self-assembly of a π gelator and fullerene derivative with photoinduced electron transfer for photocurrent generation. Langmuir 2010; 26:6669-75; (f) Xue P, Wang P, Yao B, Sun J, Gong P, Zhang Z et al. Nanofibers of hydrogen-bonded two-component gel with closely connected p- and n-channels and photoinduced electron transfer. ACS Appl Mater Interfaces 2014;6:21426-34.

22. (a) Mukhopadhyay P, Iwashita Y, Shirakawa M, Kawano S, Fujita N, Shinkai S. Spontaneous colorimetric sensing of the positional isomers of dihydroxynaphthalene in a 1d organogel matrix. Angew Chem Int Ed 2006;45:1592-5 (b) Jin Q, Zhang L, Zhu X, Duan P, Liu M, Amphiphilic schiff base organogels: metal-ion-mediated chiral twists and chiral recognition. Chem Eur J 2012;18:4916-22.

23. (a) Hong JP, Um MC, Nam SR, Hong JI, Lee S. Organic single-nanofiber transistors from organogels. Chem Commun 2009;310-2; (b) Tsai WW, Tevis ID, Tayi AS, Cui H, Stupp SI. Semiconducting nanowires from hairpin-shaped self-assembling sexithiophenes. J Phys Chem B, 2010, 114, 14778-86; (c) Stone DA, Tayi AS, Goldberger JE, Palmera LC, Stupp SI, Self-assembly and conductivity of hydrogen-bonded oligothiophene nanofiber networks. Chem Commun 2011;47:5702-4; (d) Xu J, Wang Y, Shan H, Lin Y, Chen Q, L Roy VA et al. Ultrasound-induced organogel formation followed by thin film fabrication via simple doctor blading technique for field-effect transistor applications. ACS Appl Mater Interfaces 2016;8:18991-7; (e) Marty R, Nigon R, Leite D, Frauenrath H. Two-fold odd–even effect in self-assembled nanowires from oligopeptide-polymer-substituted perylene bisimides. J Am Chem Soc 2014;136:3919-27.

24. (a) Rizkov D, Mizrahi S, Cohen S, Lev O, β-Amino alcohol selectors for enantioselective separation of amino acids by ligand-exchange capillary zone electrophoresis in a low molecular weight organogel. Electrophoresis

2010;31:3921–7; (b) Jintoku H, Takafuji M, Oda R, Ihara H. Enantioselective recognition by a highly ordered porphyrin-assembly on a chiral molecular gel. Chem Commun 2012;48:4881–3.

25. Cheng N, Hu Q, Guo Y, Wang Y, Yu L. Efficient and selective removal of dyes using imidazolium-based supramolecular gels. ACS Appl Mater Interfaces 2015;7:10258-65.
26. Okesola BO, Smith DK. Applying low-molecular weight supramolecular gelators in an environmental setting – self-assembled gels as smart materials for pollutant removal. Chem Soc Rev 2016;45:4226-51.
27. George M, Weiss RG. Molecular organogels. soft matter comprised of low-molecular-mass organic gelators and organic liquids. Acc Chem Res 2006:39:489-97.
28. Liu Y, Chen C, Wang T, Liu M. Supramolecular chirality of the two-component supramolecular copolymer gels: who determines the handedness? Langmuir 2016;32:322-8.
29. Shirakawa M, Kawano S, Fujita N, Sada K, Shinkai S, Hydrogen-bond-assisted control of H versus J aggregation mode of porphyrins stacks in an organogel system. J Org Chem 2003;68:5037-44.
30. (a) Suzuki M, Nakajima Y, Yumoto M, Kimura M, Shirai H, Hanabusa K. Effects of hydrogen bonding and van der waals interactions on organogelation using designed low-molecular-weight gelators and gel formation at room temperature. Langmuir 2003;19:8622-4; (b) Daisaku I, Masahiro S, Hirofusa S, Kenji H. Novel

Low-Molecular-Weight Gelators Based on Azobenzene Containing L-Amino Acids. Bull Chem Soc Jpn 2005;78:721–6; (c) Marchesan S, Styan KE, Easton CD, Waddington L, Vargiu AV. Higher and lower supramolecular orders for the design of self-assembled heterochiral tripeptide hydrogel biomaterials. J. Mater. Chem. B 2015;3:8123-32.

31. (a) Ajayaghosh A, Praveen VK. π-Organogels of self-assembled p-phenylenevinylenes: soft materials with distinct size, shape, and functions. Acc Chem Res 2007;40:644-56; (b) Suzuki M, Hanabusa K. L-Lysine-based low-molecular-weight gelators. Chem Soc Rev 2009;38:967-75.
32. Diosdado S, López R, Palomo C. Ureidopeptide-based brønsted bases: design, synthesis and application to the catalytic enantioselective synthesis of β-amino nitriles from (arylsulfonyl)acetonitriles. Chem Eur J 2014;20:6526-31.
33. Terech P, Weiss RG. Low molecular mass gelators of organic liquids and the properties of their gels. Chem Rev 1997;97:3133-60.
34. Weiss R G, Terech P. Molecular gels: materials with self-assembled fibrillar networks, 233–44, 2005, Springer Printed in the Netherlands.
35. Hirst AR, Coates IA, Boucheteau TR, Miravet JF, Escuder B, Castelletto V et al. Low-molecular-weight gelators: elucidating the principles of gelation based on gelator solubility and a cooperative self-assembly model. J Am Chem Soc 2008;130:9113-21.
36. Xue P, Lu R, Yang X, Zhao L, Xu D, Liu Y et al. Self-assembly of a chiral lipid gelator controlled by solvent and speed of gelation. Chem Eur J 2009;15:9824-35.

37. Zhang Y, Xue P, Yao B, Sun J. Self-assembly of azobenzene-based two-component gels. New J Chem 2014;38:5747-53.

38. Kawano S, Fujita N, Shinkai S. Quater-, quinque-, and sexithiophene organogelators: unique thermochromism and heating-free sol–gel phase transition. Chem Eur J 2005;11:4735-42.

39. (a) Weiss RG. The past, present, and future of molecular gels. what is the status of the field, and where is it going? J Am Chem Soc 2014;136:7519-30; (b) Zurcher D M, McNeil AJ. Tools for Identifying Gelator Scaffolds and Solvents. J Org Chem 2015;80:2473-9.

40. (a) Huang X, Zhao Y, Han B. Supramolecular organic network assembled from quadruple hydrogen-bonding motifs. Chem Commun, 2016, 52, 6597-600; (b) Liu X, Fei J, Wang A, Cui W, Zhu P, Li J. Transformation of dipeptide-based organogels into chiral crystals by cryogenic treatment. Angew Chem Int Ed 2017;56:2660-3; (c) Yao H, Qi M, Liu Y, Tian W. Host–guest binding-site-tunable self-assembly of stimuli-responsive supramolecular polymers. Chem Eur J 2016;22:8508-19.

41. Xue P, Wang P, Yao B, Sun J, Gong P, Zhang Z et al. Photocurrent generation of nanofibers constructed using a complex of a gelator and a fullerene derivative. RSC Adv 2015;5:75425-33.

42. Rahman M M, Czaun M, Takafuji M, Ihara H. Synthesis, Self-assembling properties, and atom transfer radical polymerization of an alkylated L-phenylalanine-derived monomeric organogel from silica: a new approach to

prepare packing materials for high-performance liquid chromatography. Chem Eur J 2008;14:1312-21.

43. Iwahara H, Kushida T, Yamaguchi S. A planarized 9-phenylanthracene: a simple electron-donating building block for fluorescent materials. Chem Commun 2016;52:1124-7.

44. (a) Wu H, Xue L, Shi Y, Chen Y, Li X, Organogels based on J- and H-type aggregates of amphiphilic perylenetetracarboxylic diimides. Langmuir 2011;27:3074-82; (b) Li X, Zhang X, Ghosh S, Würthner F. Highly fluorescent lyotropic mesophases and organogels based on j-aggregates of core-twisted perylene bisimide dyes. Chem Eur J 2008;14:8074-8.

45. (a) Yagai S, Nakajima T, Kishikawa K, Kohmoto S, Karatsu T, Kitamura A. Hierarchical organization of photoresponsive hydrogen-bonded rosettes. J Am Chem Soc 2005;127:11134-9; (b) Qiu Z, Yu H, Li J, Wang Y, Zhang Y. Spiropyran-linked dipeptide forms supramolecular hydrogel with dual responses to light and to ligand–receptor interaction. Chem Commun 2009;3342-4; (c) Borré E, Stumbé J, Bellemin-Laponnaz S, Maur M. Light-powered self-healable metallosupramolecular soft actuators. Angew Chem Int Ed, 2016, 55, 1313-7.

46. Xue P, Zhang Y, Jia J, Xu D, Zhang X, Liu X, Zhou H, Zhang P, Lu R, Takafuji M. Ihara H. Solvent-dependent photophysical and anion responsive properties of one glutamide gelator. Soft Matter 2011;7:8296–304.

1. An azobenzene-based L-valinamide derivative was found to form gels in various solvents.
2. The hydrogen bonding between amide units and π-π interaction between azobenzene moieties were confirmed to be driving force of gel formation.
3. The gel exhibits selective response to fluoride anion.